Mater. Res. Soc. Symp. Proc. Vol. 1303 © 2011 Materials Research Society
DOI: 10.1557/opl.2011.416

Nano-Flower MnO_2 Coated Graphene Composite Electrodes for Energy Storage Devices

Qian Cheng,[1,2] Jie Tang,[1,2] Jun Ma,[1] Han Zhang,[1] Norio Shinya,[1] and Lu-Chang Qin[3]

[1]National Institute for Materials Science, 1-2-1 Sengen, Tsukuba 305-0047, Japan

[2]Doctoral Program in Materials Science and Engineering, University of Tsukuba, 1-1-1 Tennodai, Tsukuba, 305-8577, Japan

[3]Department of Physics and Astronomy, University of North Carolina at Chapel Hill, Chapel Hill, NC 27599-3255, USA

ABSTRACT

Graphene, two-dimensional layers of sp^2-bonded carbon, has many unique properties. In this paper, graphene is decorated with flower-like MnO_2 nanostructures for the application in energy storage devices. The as-prepared graphene and MnO_2 nano-flowers, which were characterized by scanning electron microscopy (SEM) and transmission electron microscopy (TEM), were assembled into an asymmetric supercapacitor. The specific capacitance of the graphene electrode reached 245 F/g at a charging current of 1 mA. The MnO_2 nano-flowers which consisted of tiny rods with a diameter of less than 10 nm were coated onto the graphene electrodes by electrodeposition. The specific capacitance after the MnO_2 deposition is 328 F/g at the charging current of 1 mA with an energy density of 11.4Wh/kg and power density of 25.8 kW/kg. This work suggests that our graphene-based electrodes can be a promising candidate for high-performance energy storage devices.

INTRODUCTION

Research on supercapacitors has generated growing interests from both academia and industry in recent years. Supercapacitors are considered as a promising power storage device for backup power storage, peak power sources, and hybrid vehicles, due to their high power density, high charge and discharge rate, and long cycle life [1].

Graphene, parent of all graphitic structures ranging from graphite to carbon nanotubes and fullerenes, has become one of the most exciting topics of research in the last few years [2].This two-dimensional material constitutes a new type of nanostructured carbon comprising a single layer of carbon atoms arranged in the graphitic sp^2 bonding configuration. It is distinctly different from carbon nanotubes and fullerenes and exhibits many unique properties. Graphene and chemically modified graphene sheets have shown a high electrical conductivity [3], high surface area, and good mechanical properties comparable with or even better than carbon nanotubes [4]. In addition, graphene-based materials can be easily obtained by simple chemical processing of graphite [5]. Furthermore, the graphene-based system of individual sheets does not depend on the distribution of pores in a solid support to offer its large surface area. Instead, every chemically modified graphene sheet can “move” physically to adjust itself to the different types of electrolytes. Therefore the access to the very high surface area of graphene-based materials by

the electrolyte can be maintained while preserving the overall high electrical conductivity for the network [6-8].

To exploit the potentials of graphene-based materials for supercapacitor applications, we have coated active materials on the graphene sheets to form hybrid electrodes for the supercapacitors to further increase the specific capacitance as well as the energy density while maintaining its good power performance. Among the effective metal oxides, MnO_2 can form many polymorphs such as α-, β-, γ-, and δ-type, offering distinctive properties and wide applications as catalysts, ion-sieves, and especially as an electrode material in Li/MnO_2 and Zn/MnO_2 batteries [9-11]. There has been some work that explored the electrochemical properties of the graphene and MnO_2 composite electrode, which were synthesized by a chemical route. Yan *et al*. reported the making of graphene/MnO_2 composite materials and obtained excellent specific capacitance of 310 F/g at the scan rate of 2 mV/s. They used the reduction of permanganate by surface carbon to prepare their electrode material and needed to use a binder and conductive agent to produce their electrode [12].

In this work, we used electrochemical deposition to fabricate our electrodes since this technique can control the coating mass, thickness, and morphology of the metal oxide film by simply adjusting the applied current, bath chemistry, and temperature. In addition, we can use this method for in situ deposition of the metal oxide film, which does not require the additional processing step of adding binders and electrical conductors. Furthermore, this technique can easily be used to synthesize nano-structures that can provide a high surface area, short diffusion path in host material, and good pore structure for electrolyte access. Although the electrodeposition method has been well studied for producing nanomaterials, there has been no report of the electrochemical properties of graphene and MnO_2 composite electrodes prepared by in situ electrodeposition. We have therefore designed and fabricated a graphene/MnO_2 composite electrode by in situ anodic electrodeposition of MnO_2 on the graphene electrode as a cathode to form an asymmetric supercapacitor.

EXPERIMENTAL

Graphene oxide was synthesized using a modified Hummers method from graphite in our experiment as described in the literature [13]. We reduced the graphene oxide using hydrazine. Manganese oxide nanostructures were anodically electrodeposited from a mixture of two different solutions (0.1 M Na_2SO_4 and 0.1 M $Mn(CH_3COO)_2$) onto the graphene film using a cyclic voltammetric technique with 250 mV/s at different cycles. A platinum sheet of 20 mm × 10 mm was placed vertically 20 mm away from the working electrode as a counter electrode. An Ag-AgCl electrode was used as a reference electrode. The anode is made of graphene and cathode is made of the MnO_2-coated graphene. Both of the electrodes used a high purity titanium sheet as the current collector. The two electrodes were separated by a thin polypropylene film in a 1 M KCl aqueous electrolyte solution.

RESULTS AND DISCUSSION

Figure 1 shows the morphologies of the as-synthesized graphene and MnO_2 coated graphene. Figure 1a is a TEM image of our synthesized graphene. We can see that the few layer graphenes were usually overlapped with each other. The morphology of the as-synthesized MnO_2 nanostructures coated on the few-layer graphene is shown in Figure 1b. The graphene cannot be seen directly in the SEM image due to high-density coating of MnO_2.The MnO_2 nano-

flower consisted of many MnO_2 nano-rods as shown in Figure 1c. When examined at high resolution, as shown in Figure 1d, the as-synthesized MnO_2 nano-rods have a typical diameter of less than 10 nm and the structure of the nano rods is γ-MnO_2. The MnO_2 synthesized here may have preferentially grown on energetically favorable sites under cyclic voltammetric control, resulting in a highly porous structure that promotes efficient contact between the active material and the electrolyte, providing more active sites for electrochemical reactions. It should also be noted that structures with porosity and interconnectivity supply additional accessible space for ions while maintaining sufficient conductivity for solid-state electronic transfer. Moreover, the needle like structure can provide short diffusion path lengths to both ions and electrons and also sufficient porosity for electrolyte penetration giving rise to high charge and discharge rates [14].

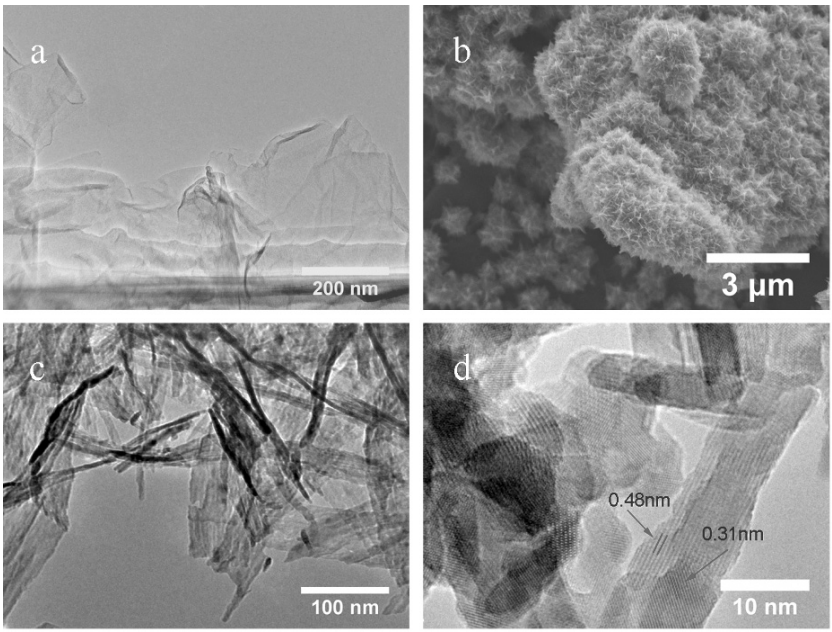

Figure 1 Morphology of graphene and MnO_2 coated graphene. (a) TEM image of graphene. (b) SEM image of MnO_2 coated graphene electrode. (c) TEM of image of MnO_2 nano-rods. (d) High resolution TEM image of MnO_2.

The pseudocapacitance of MnO_2 in aqueous neutral electrolytes is attributed to the following redox reaction

$$MnO_2 + \delta X^+ + \delta e^- \leftrightarrow MnOOX_\delta \quad (1)$$

where X^+ corresponds to H^+ or alkali metal cations such as Na^+ and K^+. On the basis of Faraday's law, the theoretical specific capacitance of the reduction of $Mn(IV)O_2$ to $Mn(III)OO_X$ is approximately 1100 F/g with a voltage window of 1.0 V [15]. The charging and discharging

curve under 1 mA of the electrode before and after the MnO_2 coating is shown in Figure 2a. Both charge and discharge times increased after the MnO_2 coating. The supercapacitor test cell is assembled as a two-electrode system which uses graphene as the anode and MnO_2-coated graphene as the cathode. The calculated specific capacitance after the MnO_2 coating is 328 F/g.

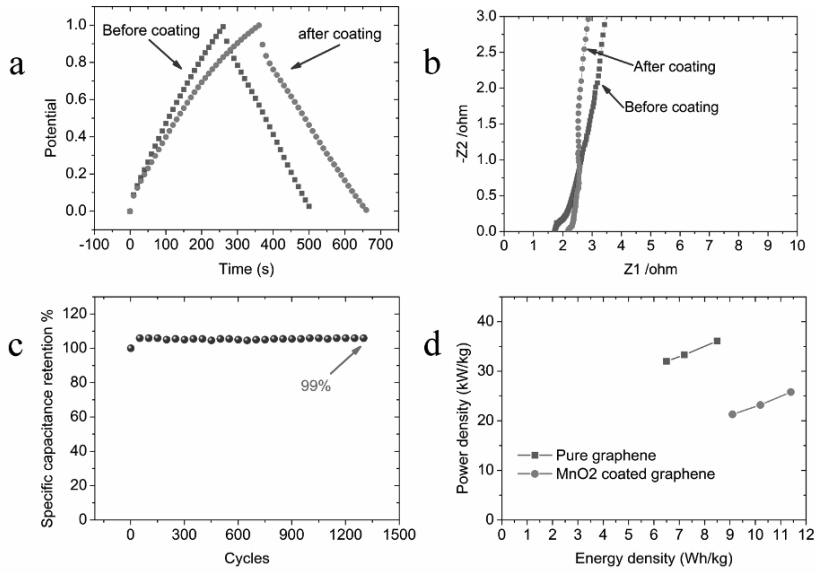

Figure 2 Electrochemical properties of graphene electrode after MnO_2 coating. (a) Comparison of charge and discharge curves before and after MnO_2 coating. (b) Nyquist plot of pure graphene and MnO_2-coated graphene electrodes. (c) Capacitance retention curve of long time cycleing in aqueous electrolyte. (d) Ragone plot of pure graphene and MnO_2 coated graphene electrodes.

The specific capacitance increased 34.4% after the MnO_2 coating. The energy density after the MnO_2 coating reached 11.4 Wh/kg. Figure 2b shows the Nyquist plots of the MnO_2-coated graphene electrode. The equivalent series resistance (ESR) is 2.2 Ω which is calculated from the x-intercept on the plot. The maximum power density is 25.8 kW/kg. The high frequency loop is from 2371 Hz to 14 Hz. The loop is quite small, indicating the small resistance between graphene and the MnO_2 nanostructures. This is because the nanostructured MnO_2 is grown on the graphene sheets electrochemically rather than formed by mechanical blending. We can also observe in the Nyquist plot that the MnO_2-coated graphene has a more straight line than graphene electrode in the low frequency region, because the direct growth of MnO_2 on graphene enlarges the separation of graphene nano-sheets resulting in a faster migration rate for the electrolyte. This effect is illustrated schematically in Figure 3. Since an ideally polarizable capacitance gives rise to a straight vertical line along the series, this line must have a finite slope to represent the diffusive resistance of electrolyte in the electrode pores and the proton diffusion in host materials. Generally this type of proton diffusion (solid-state diffusion) is slower in host

materials than in electrolyte, therefore the linearity is assumed to be the semi-infinite diffusion in solid materials. The slope of the MnO_2-coated graphene increased due to a lowered diffusion resistance by the shortened proton diffusion path. The in situ electrochemical coating method we used here could also provide a three-dimensional coating of the entire graphene electrode. The long time cycling is shown in Figure 2c. We found that the capacitance increased at the beginning of the cycling just like our graphene electrodes. It showed almost as a straight line after about 150 cycles. The capacitance only decreased by 1% after 1300 cycles, indicating an excellent cyclicity of our MnO_2-coated graphene electrodes. The ragone plot of the graphene and MnO_2 coated graphene electrodes are shown in Figure 2d.

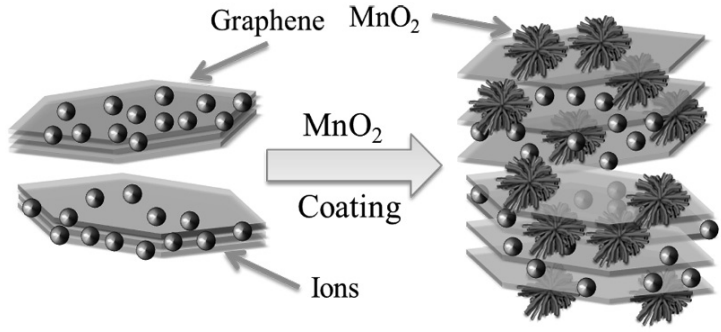

Figure 3 Schematic illustration of MnO_2 coating on graphene. The separation of graphene nano-sheets is enlarged to lead to high migration rate for electrolyte.

Both the graphene and MnO_2-coated graphene electrodes showed very good power and energy performance. The excellent properties are attributed to the high accessible specific surface area and high efficiency of the electrolytic ion absorption. Graphene sheets, single-layered or few-layered, offer an ideal structure for ion absorption. Moreover, the graphene based electrode does not depend on the exact pore distribution to give its large surface area. The graphene nano-sheet can adjust itself to different electrolytes. Therefore, access to the very high surface area of graphene materials by the electrolyte can be maintained while preserving the overall high electrical conductivity. The graphene-based electrode can also have a larger thickness than the activated carbon-based electrode. Activated carbon has a larger electrical resistance that limits the thickness and usually contains conductive but low surface area additives such as carbon black to enable rapid electrical charge transfer from the cell [6]. The high electrical conductivity of the graphene materials eliminates the need for conductive fillers and allows increased electrode thickness. Increasing the electrode thickness and elimination of additives lead to improved electrode materials for charge collection/separation. The MnO_2 nanoflowers grown on graphene nano-sheets enlarge the separation between the graphene sheets to enhance the access of the electrolyte ions, as illustrated in Figure 3, The nano-structured MnO_2 would enhance the efficiency for redox reactions and further increase the specific capacitance. Therefore the high performance of the supercapacitor electrode reported here is attributed to both graphene and the nano-structured MnO_2.

CONCLUSIONS

We have successfully fabricated binderless supercapacitors by using graphene and MnO_2 nanoflowers coated graphene to produce a high specific capacitance of 245 F/g for graphene and 328 F/g for MnO_2-coated graphene, respectively. The electrodeposited γ-MnO_2 serve as a spacer for the graphene nano-sheets, which increases the ion diffusion rate of the electrolyte. It can also improve the accessibility of the electrolyte to make full use of the electrode material. Furthermore, the fast surface redox reactions can greatly increase the specific capacitance of the electrode as well as the energy density to make such supercapacitors possible for use in electrical vehicles or hybrid vehicles. In addition, the power density of our asymmetric supercapacitor reached 25.8 kW/kg, which is well suited for high power applications.

ACKNOWLEDGMENTS

This work was supported by JSPS Grants-in-Aid for Scientific Research No.19310081 and 22310074, and the Nanotechnology Network Project of the Ministry of Education, Culture, Sports, Science and Technology (MEXT), Japan. LCQ wishes to acknowledge partial support from US Department of Energy, Office of Basic Energy Sciences as part of an Energy Frontier Research Center at the University of North Carolina at Chapel Hill.

REFERENCES

1. P. Simon and Y. Gogotsi, Nature Mater. **7**, 845-854 (2008).
2. J. C. Meyer, A. K. Geim, M. I. Katsnelson, K. S. Novoselov, T. J. Booth, and S. Roth, Nature **446**, 60-63 (2007).
3. C. Gomez-Navarro, R. T. Weitz, A. M. Bittner, M. Scolari, A. Mews, M. Burghard, and K. Kern, Nano Lett. **7**, 3499-3503 (2007).
4. H. A. Becerril, J. Mao, Z. Liu, R. M. Stoltenberg, Z. Bao, and Y. Chen, ACS Nano **2**, 463-470 (2008).
5. V. C. Tung, M. J. Allen, Y. Yang, and R. B. Kaner, Nature Nanotechnol. **4**, 25-29 (2009).
6. M. D. Stoller, S. J. Park, Y. W. Zhu, J. H. An, and R. S. Ruoff, Nano Lett. **8**, 3498-3502 (2008).
7. S. Stankovich, D. A. Dikin, G. H. B. Dommett, K. M. Kohlhaas, E. J. Zimney, E. A. Stach, R. D. Piner, S. T. Nguyen, and R. S. Ruoff, Nature **442**, 282-286 (2006).
8. A. K. Geim and P. Kim, Sci. Am. **298**(4), 90-97 (2008).
9. M. M. Thackeray, Prog. Solid State Ch **25**, 1-71 (1997).
10. B. Ammundsen and J. Paulsen, Adv. Mater. **13**, 943-956 (2001).
11. M. S. Whittingham, Chemical Reviews **104**, 4271-4301 (2004).
12. J. Yan, Z. J. Fan, T. Wei, W. Z. Qian, M. L. Zhang, and F. Wei, Carbon **48**, 3825-3833 (2010).
13. F. Ali, N. Agarwal, P. K. Nayak, R. Das, and N. Periasamy, Curr. Sci. India **97**, 682-684 (2009).
14. R. Liu and S. B. Lee, J. Am. Chem. Soc. **130**, 2942-2943 (2008).
15. S. B. Ma, K. W. Nam, W. S. Yoon, X. Q. Yang, K. Y. Ahn, K. H. Oh, and K. B. Kim, J. Power Sources **178**, 483-489 (2008).